Two models for the dynamics of boiling in a short capillary tube

A. Cordonet
Centre de Physique Théorique, CNRS, Luminy, case 907, Marseille cedex 09, France and IICO, UASLP, San Luis Potosí, 78210 México

R. Lima
Centre de Physique Théorique, CNRS, Luminy, case 907, Marseille cedex 09, France

E. Ramos
Laboratorio de Energía Solar-IIM, Universidad Nacional Autónoma de México, Ap. P. 34, 62580 Temixco (Mor.), México

(Received 18 July 2000; accepted 8 March 2001; published 27 April 2001)

We investigate the dynamical origin of the statistical properties of boiling in a short capillary tube. Two different models are proposed (Markov model and rotational model). We show that the behavior of each model may be related to different properties of the physical phenomenon. We conclude with a suggestion of a new experimental measurement which can help to adjust several aspects of the models. © *2001 American Institute of Physics.* [DOI: 10.1063/1.1368196]

Boiling dynamics presents a complex behavior, passing through chaotic, intermittent, quasi-periodic, or periodic regimes in function of the experimental parameters (heating power, capillary geometry). Despite the complex behavior observed, it is possible to characterize some statistical properties from the experimental data at each regime. The goal of the present study is to investigate the dynamical origin of the statistical features shown in experiments. Doing so, we are able to determine the relationship between each statistical indicator and the corresponding dynamical properties of our models. Our approach suggests new experimental measurements that will help to determine more features of the models.

I. INTRODUCTION

Experimental studies of boiling have revealed a great variety of qualitative behaviors. Depending on the experimental parameters the pattern of bubbles production is chaotic, intermittent, quasi-periodic, or periodic (see Ref. 1 and references therein). This variety of regimes has been extensively described and documented, but there are a number of fundamental aspects that remain unclear. In the present study we investigate the dynamical origin of the statistical features shown in experience. In doing so, we are able to determine the relationship between each statistical indicator and the corresponding dynamical properties of the models.

From the experimental sample characteristics, three statistical indicators are defined. The fact that discrete and continuous-time-like statistics are relevant leads naturally to the choice of a suspension as the model dynamical system. Once this is fixed, we consider the constraints that each statistical indicator imposes on the parameters of the models in two particular cases, the Markov model and the rotational model (to be defined later). In the first one, topological constraints are immediately imposed from data (a grammar is imposed), and we show that some correlations between the two phenomena considered are needed. The rotational model would imply long-range correlations between both processes, and is compatible with the topological constraints imposed by experimental data. The comparison of the two models suggests the consideration of other statistical indicators, such as the entropy of experimental samples, to determine which of them is most useful in modeling the process. In particular, we are faced with the question whether a mixing or a zero entropy dynamics fits better the characteristics of the experiment. This is a question that we cannot answer due to the actual lack of experimental evidence, as we shall see. Therefore, this approach suggests new experimental measurements that at the same time help to determine more features of the models. This is a characteristic of dynamical modeling. Similar methods has been used by R. Lima and E. Ugalde to model turbulence.[2,3]

In Sec. II we give a short description of the experimental arrangement. In Sec. III we define the statistical indicators that will be the bridge between the experiment and the models. The experimental behavior of the statistical indicators is described in Sec. IV. Section V is devoted to the models' description and the constraints that experimental data impose. The last section contains the conclusions.

II. EXPERIMENTAL SETUP

The experimental arrangement used to obtain the data for the present study has been described in detail before.[1] Here we give only the information required to understand the physical conditions under which the time series analyzed were obtained.

Bubbling at a chosen location in a vessel was achieved by immersing a short capillary tube (0.7 mm in diameter and 8 mm length) inside a large container (3 l) filled with distilled water at boiling temperature. The formation of vapor bubbles inside the tube is triggered by a heating wire placed at its lower end which is also sealed with ceramic paste. Supplying a small electric current to the heating wire generates water vapor that moves upwards due to buoyancy forces

and leaves the capillary tube forming bubbles. The departure of the bubbles is recorded by shining a laser beam through the water in the vessel, just above the upper end of the tube where the bubbles form and detach. In the absence of bubbles, the beam passes practically undisturbed and is recorded at the opposite end by a photo-transistor. The presence of the bubbles refracts the beam and most of the laser light deviates from the sensitive area of the photo-transistor. The output of the photo-transistor is recorded and stored digitally in a PC to be analyzed after concluding the experiment. Care was taken to use a large enough sampling rate to capture the most of the important physical events in the bubble growth and detachment process. Typically, the sensor output displays a series of peaks representing the formation and departure of trains of bubbles. The time between the departure of two consecutive bubbles can be easily recorded by determining the time between a well-defined feature of the event; for instance, the time between two maxima (or minima) in the time series.

III. STATISTICAL ANALYSIS OF THE RESULTS

For the analysis of the experimental results let us introduce three statistical indicators. The first one is simply the distribution of time intervals between two consecutive bubbles. The other two are related to the existence of two types of bubbles.

The result of an experiment is a sequence of values $\{t_i\}_{i=0}^{N}$, where t_i is the time when the ith bubble is detected. Here $N+1$ is the number of bubbles of the given experimental sequence.

Let us define the associated sequence of time intervals between bubbles as

$$\{\Delta t_i\}_{i=1}^{N}, \quad \Delta t_i = t_i - t_{i-1}. \tag{1}$$

Because of the finite experimental precision, we consider a partition $\mathcal{D}$ of the possible values of $\{\Delta t_i\}$:

$$\mathcal{D}=\{\Delta_0,\ldots,\Delta_j,\ldots\}, \tag{2}$$

where

$$\Delta t_i \in \Delta_j, \quad \text{if } j\tau \leqslant \Delta t_i < (j+1)\tau. \tag{3}$$

Here τ is at least equal to the time increments precision.

(A) We define the first statistical indicator $\eta_{\exp}(\Delta_j)$ as

$$\eta_{\exp}(\Delta_j) = \frac{\text{card}\{\Delta t_i \in \Delta_j, i=1,\ldots,N\}}{N}, \tag{4}$$

that is to say, $\eta_{\exp}(\Delta_j)$ is the experimental distribution of the time interval between two bubbles. All the experimental quantities are denoted with the subscript exp.

One observes (see Fig. 1) that for almost all the values of the experimental parameters there are two maxima in the distribution $\eta_{\exp}(\Delta_j)$. That is to say there are typically two kind of bubbles: those that appear in a short lapse of time after the preceding one (fast bubbles), and those that appear after a greater interval of time after the preceding one (slow bubble). Taking this into account we can classify the time intervals into two types: the fast ones (i.e., $\Delta t_i < \Delta_{\text{limit}}$, noted β) and the slow ones (i.e., $\Delta t_i \geqslant \Delta_{\text{limite}}$, noted α), where

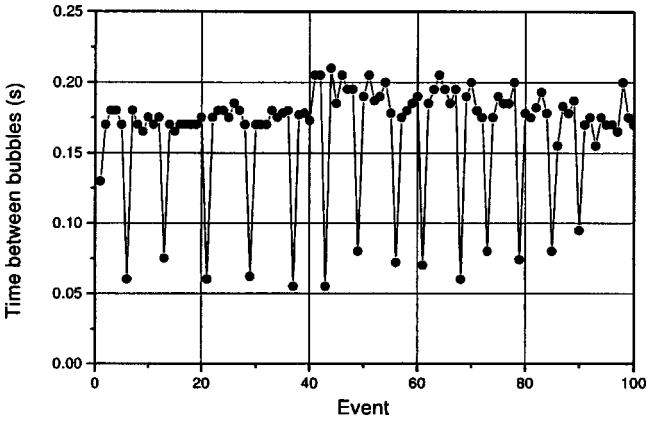

FIG. 1. Experimental sequence of the time intervals for $V=2.41$ V.

Δ_{limit} is defined in view of the experimental results (Fig. 1). This corresponds to the introduction of a partition $\mathcal{P}=\{\alpha,\beta\}$ over the values of Δt_i with

$$\begin{aligned} &\Delta t_i \in \alpha \quad \text{if } \Delta t_i \geqslant \Delta_{\text{limit}}, \\ &\Delta t_i \in \beta \quad \text{if } \Delta t_i < \Delta_{\text{limit}}. \end{aligned} \tag{5}$$

In Fig. 1 we show an experimental sequence, $V=2.41$ V, where the X axis represents the sequence $n=1,2,..,i,\ldots$ of the events (emission of the 100 first bubbles) and the Y axis the corresponding time intervals $\Delta t_i = t_i - t_{i-1}$. Fixing $\Delta_{\text{limite}}=120$ ms we obtain the symbolic sequence:

$$\omega=(\alpha,\alpha,\alpha,\alpha,\alpha,\beta,\alpha,\ldots). \tag{6}$$

It is important to remark that experimentally one cannot observe two consecutive fast bubbles. That means in symbolic terms that the block $\beta\beta$ is forbidden in ω.

(B) One introduces the second statistical indicator:

$$\nu_{\exp}[\beta] = \frac{\text{card}\{\beta \in \omega\}}{N}, \tag{7}$$

that is to say, the frequency of fast bubbles with respect to the total number of observed bubbles.

(C) The third one is defined similarly and gives the frequency of appearance of the packages of n consecutive slow bubbles:

$$\nu_{\exp}(n) = \frac{\text{card}\{\beta\overbrace{\alpha\ldots\alpha}^{n}\beta \in \omega\}}{N-n-1} \tag{8}$$

Finally, at this step, we characterize the experiment by the three statistical indicators $\eta_{\exp}(\Delta_j)$, $\nu_{\exp}[\beta]$, and $\nu_{\exp}(n)$.

The first one is defined over the possible values of the time between bubbles, and can be calculated from a partition of time units as thin as desired (i.e., one can consider a continuum of possible values of Δt_i), the only practical lower bound being the acquisition frequency of the experimental signal.

The second and third ones are defined with a discrete event space.

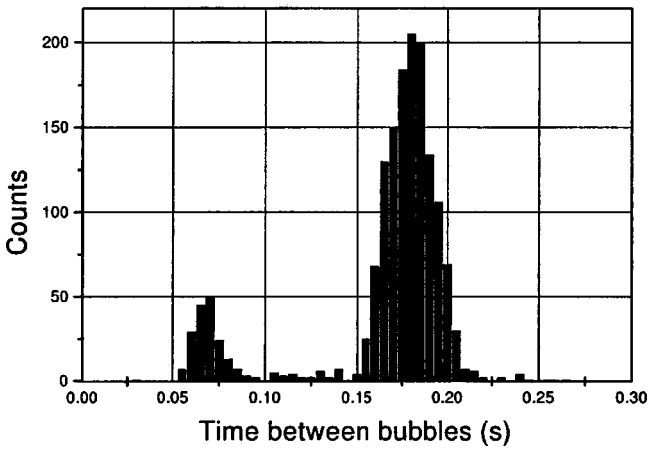

FIG. 2. card$\{\Delta t_i \in \Delta_j, i=1,...,N\}$ for $V=2.41$ V. Time unit 5×10^{-3} s.

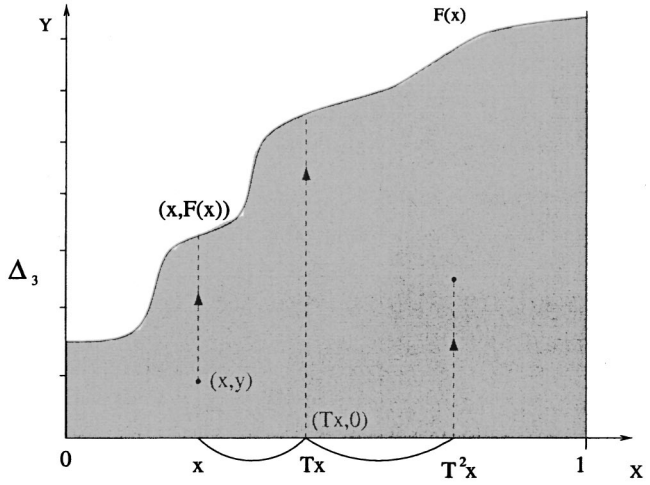

FIG. 4. Flow S_t.

IV. EXPERIMENTAL RESULTS

When the applied voltage is less than 1.0 V, there may not be bubble departure. The bubble generation experiment is performed using voltages in the rank 1–4 V. Two different behaviors, typically low and high heat rates, are identified. For low heat rates the bubbles appear in groups or packages. These packages consist mostly of 4 to 11 bubbles, departing at a constant period and separated by packages of two bubbles, leaving at a shorter period are observed. A different qualitative behavior, which is observed at larger heat rates, is an almost periodic phenomenon.

A. Low heat rates

A typical result is for 2.41 V. The histogram of the time intervals between bubbles $\Delta_j \to \eta_{\exp}(\Delta_j)$ is shown in Fig. 2. Two maxima appear for $\Delta_j = 70$ ms and $\Delta_j = 180$ ms. This result justifies the second and third statistical indicators we use. The second indicator is $\nu_{\exp}[\beta]=\frac{1}{8}$.

The distribution $n \to \nu_{\exp}(n)$ is shown in Fig. 3. The main maximum appears for $n=6$ (six consecutive slow bubbles). Two secondary maxima are detected for $n=12$ and $n=18$; the significance of these secondary maxima will be discussed later.

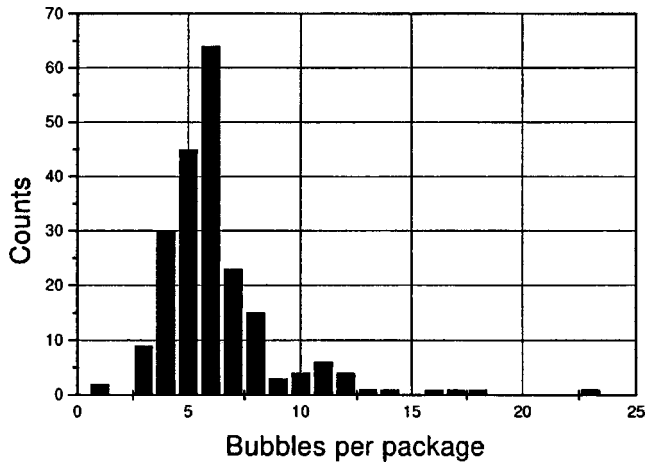

FIG. 3. card$\{\beta\overbrace{\alpha\ldots\alpha}^{n}\beta \in \omega\}$ as a function of n for $V=2.41$ V.

V. THE MODELS

A. Framework and description of the models

Because a bubble detection during the experiment can be observed at any time, it is natural to model the dynamics of the system by a flow (a continuous time dynamical system) where such an event may happen. On the other hand, we are also interested in the statistical properties of the singular events (distribution of fast and slow bubbles), and so we have to consider discrete time dynamics as well.

It is then natural to consider as a model a continuous flow allowing a Poincaré section. The dynamics of the system is described by the flow, and the events (production of bubbles) take place when the orbit passes through some surface of the phase space (the Poincaré section). Following Hopf's theorem,[4] all flow allowing such a Poincaré section is measurably isomorphic to a flow defined under a function (suspension). We give now the general description of this construction. Let T be a mapping of the unit interval and consider a function $F(x)$, $0 \leqslant x < 1$ (we shall impose some regularity to simplify the calculations); the phase space X is the area under the curve $F(x)$ for $x \in [0,1)$:

$$X=\{(x,y): 0 \leqslant x < 1, 0 \leqslant y \leqslant F(x), \text{ with the identification } (x,F(x)) \sim (Tx,0)\}. \tag{9}$$

Define over X the flow S_t, $t \in \mathbb{R}^+$:

$$S_t(x,y)=\left(T^{n(t)}x, y+t-\sum_{k=0}^{n(t)-1} F(T^k x)\right), \tag{10}$$

where $n(t)$ is uniquely fixed by

$$\sum_{k=0}^{n(t)-1} F(T^k x) \leqslant y+t < \sum_{k=0}^{n(t)} F(T^k x), \tag{11}$$

where T is a map of the interval $[0,1)$ onto itself. Actually S_t is the composition of the map T on the Poincaré section B, the base, with the flow that drives up the point (x,y) to $(x,F(x))$ at a constant velocity equal to one. This last point being identified with $(T(x),0)$, the flow goes up from this point to $(Tx,F(Tx))$, and so on (see Fig. 4).

In this framework, the emission of a bubble corresponds to the cross of an orbit through a point of the base $x \in B$, more precisely through a point $(x,0)$ of the phase space. The time between two bubbles $\Delta t_i = t_i - t_{i-1}$ is the time that the system needs to come back to the section, i.e., the return time $\tau_B(x)$ to B. In particular, this time is simply $\tau_B(x) = F(x)$.

To classify the events in slow and fast ones like in the preceding section, one can introduce a partition $\mathcal{P} = \{\alpha, \beta\}$ over B so that

$$\begin{aligned} x \in \alpha \quad &\text{if} \quad \tau_B(x) = F(x) \geqslant \Delta t_{\text{limit}}, \\ x \in \beta \quad &\text{if} \quad \tau_B(x) = F(x) < \Delta t_{\text{limit}}, \end{aligned} \tag{12}$$

where Δt_{limit} is chosen in accordance with the experiment. To take into account the fast and slow bubble production in the experiment it is natural to take F as an increasing function. This partition defines also a coding π of the map T of B to the symbolic space $\Omega \subset \{\alpha, \beta\}^{\mathbb{N}}$. An orbit $\{T^i x\}_{i=0}^{\infty}$ is coded by symbolic sequences $\omega = (\omega_0, \omega_1, \ldots)$ with $\omega_i \in \mathcal{P} = \{\alpha, \beta\}$. The dynamics over Ω is the shift σ and one has obviously

$$\pi \circ T = \sigma \circ \pi. \tag{13}$$

So, the intervals α and β are

$$\alpha = [c,1), \quad \beta = [0,c), \tag{14}$$

where $c = \inf\{x : F(x) \geqslant \Delta t_{\text{limit}}\}$.

For the dynamical invariant measure, we consider an S_t-invariant measure $\tilde{\mu} = \mu \times \xi$ with μ an ergodic measure on B, and ξ the Lebesgue measure over the orthogonal direction to B. Because of the ergodicity of μ and ξ, $\tilde{\mu}$ is also ergodic.[4] By the Birkhoff ergodic theorem, $\tilde{\mu}$ contains all the asymptotic statistical information of the model.

Concerning the relation with the statistical indicators $\nu_{\text{exp}}[\beta]$, $\nu_{\text{exp}}(n)$, and $\eta_{\text{exp}}(\Delta_j)$, we remark that these depend only on the measure μ over B and the function F. Consider first $\eta_{\text{exp}}(\Delta_j)$. It is defined as the Birkhoff sum of the experimental sequence of time intervals between bubbles $\Delta t = \{\Delta t_i\}_{i=1}^{N}$ of the observable $\chi(\Delta_j)$,[5] which is in correspondence with the measure μ over B of the model. We make the hypothesis that the experimental result is generic for the measure μ, so

$$\eta_{\text{exp}}(\Delta_j) \sim \mu(x : \tau_B(x) \in \Delta_j) = \int_{x : F(x) \in \Delta_j} d\mu(x). \tag{15}$$

For $\nu_{\text{exp}}[\beta]$ and $\nu_{\text{exp}}(n)$, following the coding of the dynamics on B modulo the partition $\mathcal{P}$, the relation with the measure μ is

$$\nu_{\text{exp}}(n) \sim \mu(\pi^{-1}[\beta \overbrace{\alpha \ldots \alpha}^{n} \beta]) = \nu([\beta \overbrace{\alpha \ldots \alpha}^{n} \beta]) \tag{16}$$

$$\nu_{\text{exp}}[\beta] \sim \nu[\beta], \tag{17}$$

where ν is the induced measure by π on Ω.[6] So, one can see that ν_{exp} depends only on the transformation T and the measure μ over the base. Here η_{exp} depends also on the function F. To be more precise, remark that ν_{exp} depends indirectly on F through the partition $\{\alpha, \beta\}$ of the base B and then on the form of F.

The properties of these three statistical indicators impose constraints on the function F and the measure μ over B that determine completely the model.

Let us examine the constraints that the experimental distribution imposes on the model.

B. Constraints imposed by $\nu_{\text{exp}}(n)$

Forgetting for the moment the time interval distribution between bubbles $[\eta_{\text{exp}}(\Delta_i)]$, let us analyze the constraints that the distribution of fast and slow bubbles $\nu_{\text{exp}}(n)$ (and $\nu_{\text{exp}}[\beta]$) imposes on the model.

We have just seen that this statistical indicator is related to the measure ν in the symbolic space Ω. It is also related to the function F because it defines the coding $\pi : B \to \Omega$.

Remark that the measure on Ω can be defined without giving an explicit form of T because only its action over the partition appears on Ω, through the shift σ.

In Fig. 2 we can see the experimental distribution $n \to \nu_{\text{exp}}(n)$ for $V = 2.41$ V.

There is at least one topological constraint that the experiment imposes; it is the impossibility of observing two consecutive fast events (fast bubbles). The largest phase space compatible with this fact is the subshift of finite type (Σ_G, σ),[6,7] defined by a grammar G:

$$G = \begin{pmatrix} 1 & 1 \\ 1 & 0 \end{pmatrix}. \tag{18}$$

It is natural to study this case first.

1. Subshift of finite type

Consider a subshift of finite type (Σ_G, σ) with grammar G. The family of ergodic measures the most natural to test are the so-called Gibbs measures (see Appendix B[2,8,9]).

A Gibbs measure is characterized by a potential ϕ. The first property that we have to fix is the rank of the potential. The next result restricts the set of accessible potentials.

Let $\phi \in \Phi_r$ be an Hölder potential of rank r, defined over Σ_G. The measure of the cylinder family $[\beta \overbrace{\alpha \ldots \alpha}^{n} \beta]$, $\nu_\phi(n)$ is a strictly decreasing function of n for $n \geqslant r-1$. Moreover, we have

$$\nu_\phi(r+k-1) = e^{ak} \nu_\phi(r-1), \quad k = 0,1,\ldots, \tag{19}$$

with

$$a = \phi(\overbrace{\alpha \ldots \alpha}^{n}) \tag{20}$$

and

$$\nu_\phi(r-1) = e^{\phi(\beta \overbrace{\alpha \ldots \alpha}^{r-1})} e^{\phi(\overbrace{\alpha \ldots \alpha}^{r-1} \beta)} \nu(\overbrace{\alpha \ldots \alpha}^{r-2} \beta). \tag{21}$$

This result implies that the rank of potential of the model is greater than or equal to the greater value of n for which $\nu_{\text{exp}}(n)$ rises a maximum. For example, after Fig. 2, and considering only the main maximum $(n = 6)$, we have to choose the potential rank at least equal to 7.

Up to here, we can see the difficulties of the model. The main difficulty that the Gibbsian model presents is that experimentally one observes the values of n for which $\nu_{\text{exp}}(n)$ has a maximum which is a function of the physical parameters (V). This implies that either we choose the potential

rank to be the maximum value of n such that $\nu^V_{\exp}(n)$ gives rise to a maxima or the rank of the potential depends on V.

In the first case the potential rank must be at least 7 (see Fig. 3) and, even if one can find the parameters of the models to fit the experimental results, the model becomes heavy and hard to handle. The second option is even worse, because the dependence of the potential rank of the physical parameters is not very natural from a physical point of view.

We are going to define a second model in Sec. V C that takes into account the secondary maxima.

Remark 1: In this case the absolutely continuous measure with respect to the Lebesgue measure (maximal entropy measure) gives the following result:

$$\nu_{\psi}(n)=(\tfrac{1}{2})^n\tfrac{1}{3}. \tag{22}$$

It is obvious that it does not reproduce the experimental data.

C. Rotational model

Consider an irrational rotation of angle θ as an automorphism over B:

$$R_\theta x=\{x+\theta\}, \tag{23}$$

where $\{z\}$ means the fractional part of z.

Consider the coding defined by the partition $\mathcal{P}=\{[0,c),[c,1)\}=\{\beta,\alpha\}$ with $c\leqslant\theta$.

This coding is compatible with the topological constraint that forbids the sequence $\beta\beta$. However, it presents other topological constraints. In particular, the complexity[10] is asymptotically equal to $p(n)=2n$ for c, and θ rationally independent and n great enough.[11] Remark that this behavior is related to the topological rigidity present in the irrational rotations. Another result that is very useful for us is the three-gaps theorem[12] (see Appendix A).

The rotations also present metric rigidity; the Lebesgue measure is the only invariant measure on the basis B. Thus, the parameters of the models are the angle of rotation θ and the value c that defines the partition.

The value of c is fixed by the experimental value of $\nu_{\exp}[\beta]$. Indeed, because the Lebesgue measure is the only invariant one, the measure of the cylinder $[\beta]$ is $\nu[\beta]=l_x(\pi^{-1}[\beta])=c$ after the coding defined by $\mathcal{P}$.

By the three-gap theorem, the measure of the family of cylinders $[\beta\overbrace{\alpha\ldots\alpha}^{n}\beta]$, is different from zero for only three values of n (n_1-1, n_2-1, and n_1+n_2-1), the three possible return times to $[0,c)$.

Thus we can reproduce the experimental maxima of $\nu_{\exp}[n]$, but they are delta peaks, which is in contradiction with the experiment.

Besides, the rotational model presents the advantage that we can adjust the values of n_1 and n_2, and, as a consequence $\nu(n)$, changing the rotational angle. That is to say, we have always $n_1=\inf\{m:\{m\theta\}\leqslant c\}$ and $n_2=\inf\{m:\{m\theta\}>1-c\}$. So, we can calculate the dependence in V of θ and c.

For example, for the case $V=2.41$ V, the experimental value of $\nu_{\exp}[\beta]\sim\frac{1}{8}$ imposes the parameter value c to be $c=\frac{1}{8}$. Besides, the experimental values of n_1 and n_2 are

$$n_1=7,\quad n_2=13. \tag{24}$$

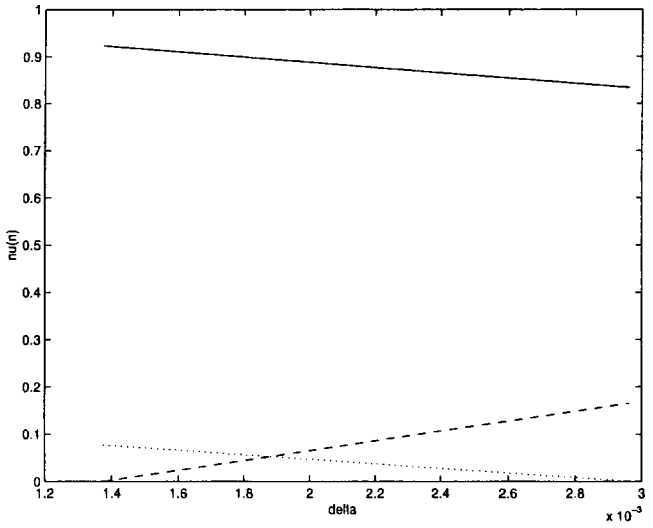

FIG. 5. $-\nu(n_1-1)--\nu(n_2-1)$ and $\ldots\nu(n_1+n_2-1)$.

These values impose a constraint on the rotational angle:

$$\theta=\tfrac{1}{7}+\delta \tag{25}$$

with

$$\frac{1}{13\cdot7\cdot8}<\delta<\frac{1}{6\cdot7\cdot8}\quad \delta\in\mathbb{R}\backslash\mathbb{Q}. \tag{26}$$

The three curves in Fig. 5 show the dependence of $\nu(n_1-1)$, $\nu(n_2-1)$, and $\nu(n_1+n_2-1)$ on δ; for $\delta=1.6\times10^{-3}$, they do agree with the weight of the three experimental picks (see Fig. 2).

D. Constraints imposed by $\eta_{\exp}(\Delta_j)$

The experimental values of the statistical indicator $\eta_{\exp}(\Delta_j)$ implies that the F function takes its values mostly in two intervals I_α and I_β:

$$\begin{aligned} &F(x)\in I_\alpha=[\Delta_{\alpha_{\min}},\Delta_{\alpha_{\max}}]\quad \text{with}\ \ \Delta_{\alpha_{\min}}\geqslant\Delta_{\lim},\\ &F(x)\in I_\beta=[\Delta_{\beta_{\min}},\Delta_{\beta_{\max}}]\quad \text{with}\ \ \Delta_{\beta_{\max}}<\Delta_{\lim}. \end{aligned} \tag{27}$$

For the $V=2.41$ V experience we choose $\Delta_{\lim}=0.12$ s.

The exact form of F that fits the results depends on the measure. Let us consider the two models.

1. Subshift of finite type

For the subshift of finite type (Σ_G,σ) with a Gibbs measure ν_ϕ the relationship between $\eta(\Delta_j)$ and F is after (15):

$$\eta(\Delta_j)=\mu_\phi(F^{-1}(\Delta_j))=\int_{x:F(x)\in\Delta_j}d\mu_\phi. \tag{28}$$

To calculate this integral we can impose an additional condition on F such that the intervals $\{x:F(x)\in\Delta_j\}$ take a cylindric form after the coding $\pi:B\to\Omega$. Then, $\eta(\Delta_j)$ can be expressed as a function of the cylinders measure. Take $F(x)\in\Delta_j:x\in\pi^{-1}([\alpha_0\alpha_1\cdots\alpha_{n-1}])$. Then

$$\eta(\Delta_j)=\nu_\phi([\alpha_0\alpha_1\cdots\alpha_{n-1}]). \tag{29}$$

In the particular case of maximal entropy measure introduced in (1) we have

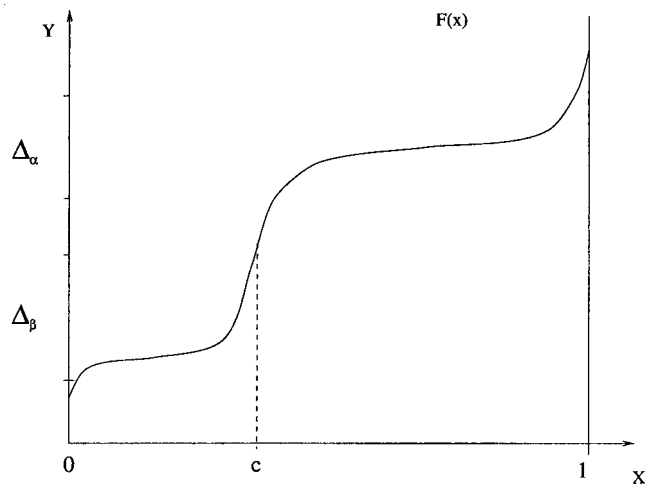

FIG. 6. $F(x)$.

$$\eta(\Delta_j)=\nu_\psi([\alpha_0\alpha_1\cdots\alpha_{n-1}])=(\tfrac{1}{2})^{n-1-\#\beta}\nu_\psi[\alpha_{n-1}], \tag{30}$$

where $\#\beta$ is the cardinality of β in $[\alpha_0\alpha_1\cdots\alpha_{n-1}]$, $\nu_\psi[\alpha]=\frac{2}{3}$, and $\nu_\psi[\beta]=\frac{1}{3}$.

2. Rotations

This case is simpler than the subshift model because the only invariant measure on the basis is the Lebesgue measure. Take the partition $\mathcal{D}=\{\Delta_1\Delta_2,\ldots\}$ over the values of $F(x)$, with

$$\Delta_j=[y_{j_{\min}},y_{j_{\max}}). \tag{31}$$

Recall that F is an increasing function:

$$\begin{aligned}\eta(\Delta_j)&=l_x(F^{-1}(\Delta_j))\\&=\int_{x:F(x)\in\Delta_j}dl_x\\&=\inf\{x:F(x)=y_{j_{\min}}\}-\inf\{x:F(x)=y_{j_{\max}}\}.\end{aligned} \tag{32}$$

For all the values of V $\eta_{\exp}(\Delta_j)$ can be reproduced by a function of the form given in Fig. 6.

VI. CONCLUSIONS

The dynamical system corresponding to the two models discussed in this article is a flow allowing a Poincaré section B. In this way, we identify the production of the bubbles with the times when the orbit crosses B. We have seen that the return time statistics to B can be described by the edge function F. Besides modeling the dynamics in B, we have found that a Gibbsian model has practical (too high potential rank) and physical problems (dependence of the rank of the potential with V). The problem of studying infinite rank potentials or non-Gibbsian measures remains open.

For the rotational model its success depends on the existence of the secondary maxima of $\nu_{\exp}(n)$ that would appear in longer observations. Additionally, the problem of finding a perturbation to the rotation in such a way that the delta peaks become wide remains open.

At present, none of the models describes completely the experimental data. However, the fact that the experimental results show some properties of each one of them means that the physical phenomenon is in some sense the superposition of two different phenomenon. Remark that the subshift model implies that the production of slow and fast bubbles is decorrelated. On the other hand, a model based on the rotations implies an important correlation between both phenomenon. Indeed, from the experimental observations (see Ref. 1) it is known that the slow bubbles appear by the accumulation of air at the bottom of the capillary tube, which leaves it after attending a critical size. To observe fast bubbles, it is necessary that a thin layer of water divides the forming bubbles into two small ones, which will leave the capillary tube within a very small interval between them. If this process appears as a consequence of the regularity of some physical magnitudes, say temperature, pressure, etc., around the capillary tube, then the rotational model may be the most natural one. On the other hand, a Gibbs model implies that this process is generated mostly random as a consequence of turbulence, instabilities or fluctuations of pressure, temperature, etc., around the capillary and therefore would be a natural candidate for a randomlike origin of the phenomena (irregularities or noise, for instance). Thus, understanding which of the models is more likely to fit the statistical properties of the phenomenon would offer us nontrivial physical information about the phenomenon. In other words, we would want to know where a mixing or a zero entropy dynamical system is the more appropriate choice regarding the experimental properties of the physical situation under consideration. Unfortunately, for the moment, our data is not enough to exclude one of the two previous scenarios.

The main issue in deciding which of the two models, or some interpolation, is the more convenient to describe the experimental situation is the analysis of the correlation times of slow and fast bubbles. In order to have a definitive answer to this alternative, longer runs in the experiment are clearly needed. This constitutes work in progress.

ACKNOWLEDGMENTS

E.R. wants to thank Guillermo Hernandez-Cruz, Raul Rechtman, and Hector Perales for obtaining the experimental data and discussions. Part of this study was financed by CONACyT (México) through project G0044E. A.C. and R.L. are grateful to the ZIF project *The Sciences of Complexity* for kind support, and R.L. is grateful to ECOS-Nord and the ZIF project.

APPENDIX A: THREE-GAP THEOREM

A well-known result in the theory of dynamical systems is the three-gap theorem:

Theorem 1 (Three gap theorem):[12] *Let θ be an irrational number in $]0,1[$ and let $\beta\in]0,\frac{1}{2}[$. The gaps between the successive integers j such that $\{\theta_j\}<\beta$ take at most three values, one being the sum of the other two. The three values $(n_1,\ n_2,$ and $n_1+n_2)$ and their asymptotic frequency are*

$$n_1=\min\{n:\{n\theta\}\in[0,\beta)\},\quad \nu_{n_1}=\beta-\{n_1\theta\},$$
$$n_2=\min\{n:\{n\theta\}\in[1-\beta,1)\},\quad \nu_{n_2}=\beta-1+\{n_2\theta\},\tag{A1}$$
$$n_1+n_2,\quad \nu_{n_1+n_2}=\{n_1\theta\}+1-\{n_2\theta\}-\beta.$$

Because of the uniqueness of the invariant measure this result is still true in terms of return times to all set of the type $[a,b)$, and for all initial condition.

APPENDIX B: GIBBS MEASURES

In this appendix, we deal with the construction of a class of σ-invariant ergodic measures that impose the frequencies of the admissible cylinders, namely Gibbs measures. In particular, this class contains Bernoulli and Markov measures. We will state the basic definitions and results of thermodynamic formalism.

A potential ϕ is a continuous function from Σ to $\mathbb{R}$. In the case when Σ_G is a subshift, we still denote by ϕ its restriction to Σ_G. ϕ is said to be Hölder continuous if $\mathrm{var}_n\phi\leqslant C_\phi d(\omega,\omega')^n=C_\phi\theta^n(C_\phi>0)$, where $\mathrm{var}_n\phi \overset{\text{def}}{=}\sup\{|\phi(\omega)-\phi(\omega')|:\omega_j=\omega'_j,0\leqslant j<n\}$.[13]

The topological pressure of ϕ on Σ_G is denoted by $P_{\Sigma_G}(\phi,\sigma)$ and defined as follows:

$$P_{\Sigma_G}(\phi,\sigma)\overset{\text{def}}{=}\lim_{n\to\infty}\frac{1}{n}\log \times\sum_{\substack{a_{0:n-1}\\ [a_{0:n-1}]\cap\Sigma_G\neq\emptyset}}\exp(S_n\phi[a_{0:n-1}]),\tag{B1}$$

where $S_n\phi[a_{0:n-1}]\overset{\text{def}}{=}\sup\{S_n\phi(\omega):\omega_{0:n-1}=a_{0:n-1}\}$ and $[a_{0:n-1}]$ is the shorthand notation for $[a_0,a_1,\ldots,a_{n-1}]$.

The ''Gibbs inequality'' characterizes Gibbs measures by giving the approximate measure of *any admissible* cylinder. This is stated in the next Theorem. We will use the shorthand notation $a\sim c^{\pm}b$ to mean $c^{-1}b\leqslant a\leqslant cb$.

Theorem 2: *Let ϕ be a Hölder continuous potential and Σ_G a subshift of finite type. Then there exists a unique σ-invariant probability measure μ_ϕ such that there exists a constant C_ϕ, such that for any $\omega\in\Sigma_G$ and any $n\geqslant 1$, we have*

$$\mu_\phi[\omega_{0:n-1}]\sim C_\phi^{\pm}\exp(-nP_{\Sigma_G}(\phi,\sigma)+S_n\phi(\omega)).\tag{B2}$$

If $[a_{0:n-1}]$ is not Σ_G-admissible, then we set $\mu_\phi[a_{0:n-1}]=0$. We should write $\mu_\phi^{\Sigma_G}$ instead of μ_ϕ if there is an ambiguity on the space where the measure is defined.

Gibbs measures are ergodic (in fact, they have strongly mixing properties).

A Gibbs measure can be characterized as an equilibrium state of the potential ϕ as follows. There is a unique σ-invariant measure for which the supremum of $h(\eta)+\int_{\Sigma_G}\phi\,d\eta$ over all σ-invariant measures η (defined on Σ_G) is attained and equal to $P_{\Sigma_G}(\phi,\sigma)$, namely the measure μ_ϕ. $h(\eta)$ is the metric entropy of η.

The Gibbs inequality previously stated gives a characterization of Gibbs measures with cylinders. The transfer operator (sometimes called the Ruelle–Perron–Frobenius operator) characterizes them as the solution of an eigenvalue problem. Define $\mathcal{L}_\phi$ acting on any continuous function f as follows:

$$(\mathcal{L}_\phi f)(\omega)\overset{\text{def}}{=}\sum_{\substack{\omega':\sigma\omega'=\omega\\ \omega'\in\mathcal{S}}}\exp(\phi(\omega'))f(\omega').\tag{B3}$$

This operator is linear, positive, and bounded in the $\|.\|_\infty$-norm.

The so-called ''Ruelle–Perron–Frobenius'' theorem asserts the following: $\mathcal{L}_\phi$ has a unique positive eigenfunction r_ϕ associated with the eigenvalue $\lambda=\exp(P_{\Sigma_G}(\phi))$, which is simple and maximal. The dual operator $\mathcal{L}_\phi^*$ has the probability measure ν as unique eigenvector, with the same eigenvalue λ. The Gibbs measure μ_ϕ is equal to $r_\phi\nu$.

[1] E. Ramos, P. Parmanada, G. Hernández-Cruz, and M. Sen, ''Dynamics of boiling from a short capillary tube,'' Exp. Heat Transfer **10**, 273–290 (1997).

[2] E. Ugalde and R. Lima, ''On a discrete dynamical model for local turbulence,'' Physica D **95**, 144–157 (1996).

[3] E. Ugalde, ''Self-similarity and finite-time intermittent effects in turbulent sequences,'' J. Phys. A **29**, 4425–4443 (1996).

[4] I. P. Cornfeld, S. V. Fomin, and Y. G. Sinai, *Ergodic Theory* (Springer-Verlag, New York, 1982).

[5] $\chi(\Delta_j)=1$ if $\Delta t_1\in\Delta_j$, 0 otherwise.

[6] A. Katok and B. Hasselblatt, *Introduction to Modern Theory of Dynamical Systems*, Encyclopedia of Math. and its Applications, Vol. 54 (Cambridge University Press, Cambridge, 1995).

[7] $\Sigma_G=\{\omega=(\omega_0,\omega_1,\ldots):G_{\omega_i\omega_{i+1}}=1\forall i\}$.

[8] R. Bowen, ''Equilibrium states and the ergodic theory of Anosov diffeomorphisms,'' *Lecture Notes in Mathematics* 470 (Springer-Verlag, New York, 1975).

[9] J. R. Chazottes, E. Floriani, and R. Lima, ''Relative entropy and identification of Gibbs measures in dynamical systems,'' J. Stat. Phys. **90**(3/4), 697–725 (1998).

[10] The complexity $p(n)$ of a symbolic space is the cadinality of different sequences of length n that can be observed in any sequence ω corresponding to an experimental series.

[11] J. Berstel, ''Recent results in Sturmian words,'' in *Developments in Language Theory II*, Magdeburg 1995 (World Scientific, Singapore, 1996), pp. 13–24.

[12] N. Slater, ''Gaps and steps problems for the sequence $n\theta$ mod 1,'' Proc. Cambridge Philos. Soc. **63**, 115–137 (1967).

[13] Notice that all results concerning a Hölder continuous potential ϕ remain valid in the weaker situation when $\Sigma_n\mathrm{var}_n\phi<\infty$.